

Influence of the equation of state on the compression and heating of hydrogenN. A. Tahir,¹ H. Juraneck,² A. Shutov,³ R. Redmer,² A. R. Piriz,⁴ M. Temporal,⁴ D. Varentsov,⁵ S. Udrea,⁵
D. H. H. Hoffmann,^{5,6} C. Deutsch,⁷ I. Lomonosov,³ and V. E. Fortov³¹*Institut für Theoretische Physik, Universität Frankfurt, Postfach 11 19 32, 60054 Frankfurt, Germany*²*Universität Rostock, Fachbereich Physik, 18051 Rostock, Germany*³*Institute for Problems in Chemical Physics Research, Chernogolovka, Russia*⁴*E.T.S.I. Industriales, Universidad de Castilla-La Mancha, 13071 Ciudad Real, Spain*⁵*Institut für Kernphysik, Technische Universität Darmstadt, Schlossgarten Strasse 9, 64289 Darmstadt, Germany*⁶*Gesellschaft für Schwerionenforschung, Planckstrasse 1, 64291 Darmstadt, Germany*⁷*Laboratoire de Physique des Gaz et des Plasmas, Université Paris-Sud, 91405 Orsay, France*

(Received 23 December 2002; published 5 May 2003)

This paper presents two-dimensional hydrodynamic simulations of implosion of a multilayered cylindrical target that is driven by an intense heavy ion beam which has an annular focal spot. The target consists of a hollow lead cylinder which is filled with hydrogen at one tenth of the solid density at room temperature. The beam is assumed to be made of 2.7-GeV/u uranium ions and six different cases for the beam intensity (total number of particles in the beam, N) are considered. In each of these six cases the particles are delivered in single bunches, 20 ns long. The simulations have been carried out using a two-dimensional hydrodynamic computer code BIG-2. A multiple shock reflection scheme is employed in these calculations that leads to very high densities of the compressed hydrogen while the temperature remains relatively low. In this study we have used two different equation-of-state models for hydrogen, namely, the SESAME data and a model that includes molecular dissociation that is based on a fluid variational theory in the neutral fluid region which is replaced by Padé approximation in the fully ionized plasma region. Our calculations show that the latter model predicts higher densities, higher pressures but lower temperatures compared to the SESAME model. The differences in the results are more pronounced for lower driving energies (lower beam intensities).

DOI: 10.1103/PhysRevB.67.184101

PACS number(s): 51.50.+v, 51.60.+a, 51.70.+f

I. INTRODUCTION

Hydrogen is the simplest and the most abundant material in the universe. A study of this element under extreme conditions of density and pressure is of great importance to astrophysics, planetary sciences and inertial fusion. Another very interesting outcome of the research carried out in this field has been the prediction in 1935 by Wigner and Huntington¹ that an insulator-to-metal transition may occur when the normal molecular hydrogen is subjected to a pressure of 0.25 Mbar.

Due to substantial technological advances in the field of high-pressure physics during the past few decades, research in this field has progressed significantly. Static as well as transient ultra-high pressures have been applied to compress samples of hydrogen and deuterium. The most popular technique to create the first type of pressure is that of employing a diamond anvil cell^{2,3} while the gas guns,^{4,5} explosives^{6,7} and high power lasers^{8,9} have been used to generate the latter type of pressure. As a result of this work, significant progress has been made in understanding the properties of high-energy-density (HED) states of hydrogen, but the final goal of creating monoatomic metallic solid hydrogen has not yet been achieved.

In a previous paper¹⁰ we showed with the help of two-dimensional hydrodynamic simulations that an intense heavy ion beam can be employed as an efficient tool to induce HED states in hydrogen. It was demonstrated that using an appropriate beam-target geometry one may employ a multiple shock reflection scheme which would lead to a low entropy

compression of hydrogen, leading to the theoretically predicted physical conditions for hydrogen metallization. In these calculations we started the implosion using solid hydrogen at an initial temperature of 10 K. These metallization conditions include a density of about 1 g/cm³, a pressure of the order of 5 Mbar and a temperature of a few thousand K. The SESAME equation-of-state (EOS) data¹¹ were used in the above calculations. However significant differences have been reported between the experimental results obtained by laser-driven shock wave experiments¹² and the calculational results achieved by using the SESAME data. It is possible that one need to improve the physical models used in SESAME so that the experimental measurements and the theoretical calculations come to a reasonable agreement. In order to study the sensitivity of the simulation results to the EOS model, we have carried out calculations using an EOS model for hydrogen that includes a dissociation model for the neutral fluid region^{13,14} which is supplemented with Padé approximations (PAs) (Ref. 15) for the fully ionized plasma region. However, we do not have a suitable EOS model to represent the solid phase of hydrogen at very low temperatures. Therefore for the purpose of comparison between the two EOS models we assume that the target is composed of hydrogen at one tenth of the solid density (0.00883 g/cm³) at room temperature. These simulations have been carried out using a two-dimensional hydrodynamic code, BIG-2.¹⁶ The beam parameters used in this study are that of the the beam which will be available at the future heavy ion synchrotron facility (SIS100) at the Gesellschaft für Schwerionenforschung (GSI), Darmstadt.

These simulations have demonstrated that our EOS for hydrogen shows a softer behavior than the SESAME EOS. Using our model one achieves a higher density, a higher pressure but a lower temperature compared to that obtained using the SESAME data. These differences are more pronounced for low driving energies while for higher driving energies the two EOS models seem to give similar results. These results suggest that the treatment used for molecular dissociation in the fluid variational theory (FVT) and the treatment used for atomic ionization in the PA require more energy compared to the respective treatments of these processes in the SESAME EOS.

Experiments are being planned to investigate HED states in matter induced by heavy ion beams at the future SIS100 facility. One of these experiments will be to perform low entropy compression of hydrogen to study the EOS properties of this important material under extreme conditions including an investigation of an insulator-to-metal transition. We believe that the simulations presented in this paper will be very helpful in designing such experiments.

Using the existing SIS18 accelerator facility at the GSI, interesting experimental work has already been done at the GSI using materials including rare gas cryogenic targets and lead.^{17–19} In Sec. II we describe our new EOS model for hydrogen while the beam and target parameters used in these calculations are given in Sec. III. The simulation results are presented in Sec. IV and the conclusions drawn from this work are noted in Sec. V.

II. EQUATION OF STATE FOR HYDROGEN

In this section we describe the equation of state models for hydrogen that we have used to carry out the compression simulations presented in this paper.

The deviations of the laser-driven shock-wave experimental results¹² from the Hugoniot curve derived from the standard SESAME EOS (Refs. 11 and 20) have initiated extensive research for an improved hydrogen EOS that fits better to the Nova laser experimental data, see for example.^{21,22}

As an alternative to the SESAME EOS, we have chosen an EOS which has the following features: (i) for the neutral fluid it includes a dissociation model^{13,14} based on a fluid variational theory, (ii) for the plasma state it uses Padé approximations,¹⁵ and (c) Between the FVT and the PAs the mass action law determines the fraction of neutral atoms and molecules and the charged particles electrons and ions.

This combined EOS which is composed of FVT and PAs (FVT/PA) leads to physical conditions that are closer to the Nova laser experiment results while the SESAME EOS reproduces the most recent Z-pinch machine experimental measurements.²³ It is therefore important to study these two EOS models over a wider range of parameters than that covered by the above two experiments and compare the results. This range of parameters will be accessed by the future SIS100 heavy ion facility at the GSI. A detailed description of the SESAME EOS can be found in Ref. 20 while a brief description of the FVT/PA is presented below.

The dissociation models for the neutral fluid region so far show one of the best agreements with the recent compression

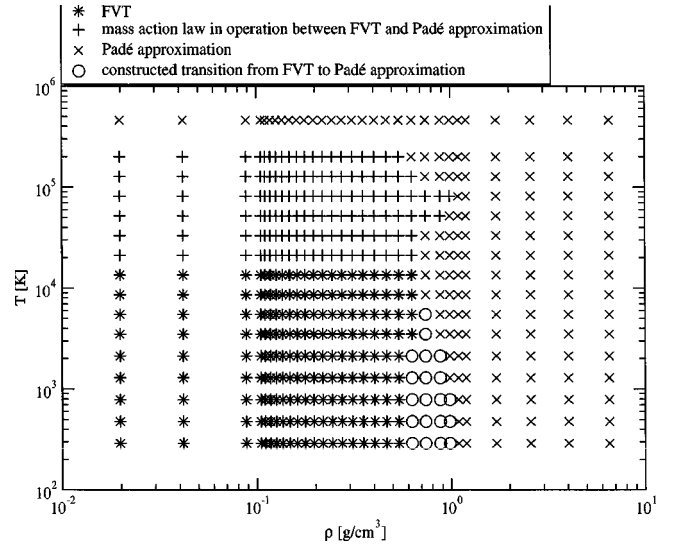


FIG. 1. An overview of the hydrogen EOS data grid. Symbols denote the effective theory at the data points.

experiments in the pressure region of up to 1 Mbar. Our dissociation model is based on the fluid variational theory (FVT) that was developed for hydrogen by Ross.²⁴ We have extended this FVT to a system of neutral atoms and molecules¹⁴ and consider dissociation $H + H \rightleftharpoons H_2$, which suggests the name dissociation model. The hydrogen atoms and molecules interact via effective pair potentials of the exp-6 form which are used in the FVT together with a hard sphere reference system²⁵ to calculate the free energy. Since in this approach the free energy depends on density and temperature, it is a thermodynamic potential and can be used to derive all other thermodynamic quantities including pressure, internal energy, and sound velocity.

In the meanwhile, more accurate PAs for the fully ionized plasma²⁶ have been developed and are used in this work instead of the former ones used in Refs. 27 and 28. These PAs show one of the best agreements with the Nova laser shock experiments in the upper pressure region above 1 Mbar as shown in Ref. 13.

In Fig. 1 is shown which theory was chosen at each specific data point on the density and temperature grid. The different symbols indicate the chosen model. The crosses \times symbolize the PA while the stars \star represent the FVT. Using the mass action law we could easily construct a transition from the FVT to the PA. The data points with a plus sign represent the region where this method has been applied. The method failed at the data points with circles and there we constructed a transition from the FVT to the PA. Higher accuracy in the region of the circles was not required since the simulation results did not access this region.

Our EOS thus describes hydrogen starting from a neutral molecular fluid going through the processes of dissociation and ionization as the density and temperature of the sample increase. At low and moderate temperatures molecules and atoms as well as electrons and protons coexist, but at temperatures of the order of 15 000 K the fraction of fully ionized hydrogen increases strongly with increasing density and temperature. This leads to a substantial increase in the elec-

trical conductivity of the sample. It has also been shown²⁹ that a significant increase in the electrical conductivity may take place even at much lower temperatures in a region dominated by the neutral fluid as a result of the so-called “hopping processes.”

At temperatures below 15 000 K especially in the region with the circle data points in Fig. 1, the model suggest a phase transition. This region is not entered by this simulation when we start compression in the neutral fluid instead of starting from solid hydrogen. Nevertheless experimentally determined conductivities above 15000 K could show if the chemical model predicts the conductivities correctly. If this would be the case, it will allow for a conclusion for a possible plasma phase transition.

The initial estimate of 0.25 Mbar proposed by Wigner and Huntigton¹ in 1935 for the hydrogen metallization pressure were followed by predictions using more accurate plasma models.^{27,30,31} These calculations show that the metallization region is extremely sensitive to the approximations and assumptions used in the models. Only the experiments will be able to give an accurate answer if and where the phase transition occurs.

Although a pressure of 3 Mbar has been achieved in DAC experiments,^{2,3} metallization could not be verified. The dynamic experiments that are done employing transient pressures have proved to be more successful. Single shock as well as multiple shocks were performed with high-intensity lasers^{8,9} and gas guns.^{4,5} In the gas gun experiments, a four orders of magnitude increase in the electrical conductivity of fluid hydrogen was observed after the sample was subjected to multiple shocks that lead to a pressure of 1.4 Mbar at a temperature of 3000 K. Laser-driven single shocks show a substantial increase in reflectivity related to a metallic-like state.⁸

In explosive driven multiple shock experiments,^{6,7} hydrogen samples have been subjected to pressures of the order of 1.5 Mbar. An abrupt increase in the electrical conductivity of the material which is close to the values of a liquid metal, has been observed at densities of 0.5 g/cm³.

The problem of shock experiments is the strong temperature increase which prevents a compression to higher densities. It is known that nearly isentropic shock compressions have the lowest temperature increase and, therefore, can achieve higher densities where the plasma phase transition is expected to occur.

We therefore proposed¹⁰ that intense heavy ion beams can be a very effective additional tool to study this important problem. Heavy ion beams have a number of advantages compared to the above methods. For example, the heavy ions can uniformly heat extended volumes of matter which can provide a much larger sample of compressed hydrogen. Moreover, the ion energy is directly coupled to the material and one does not have to rely on material ablation to drive the shocks. This makes the heavy ion driven system very efficient and one can achieve much higher densities and pressures. Slow heavy ion driven implosion ensures a low entropy compression of the material. The time scale for heavy ion heated systems is of the order of 100 ns, which is short enough to avoid any significant diffusion of hydrogen

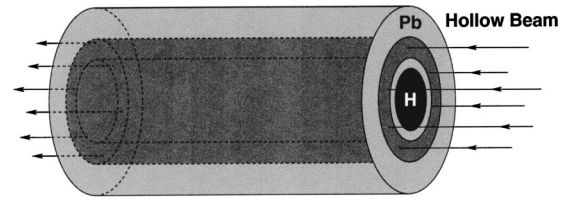


FIG. 2. Initial conditions of a heavy-ion imploded multilayered target for hydrogen metallization experiment.

through the walls of the containing cell and yet long enough to carry out experimental investigation.

The purpose of these simulations is to compare the implosion results using two different EOS models and to investigate to what regions of the hydrogen phase diagram these models lead to. This information will be very helpful to understand the results of the experiments that will be carried out at the GSI at the future SIS100 facility.

III. BEAM-TARGET GEOMETRY AND PARAMETERS

The beam-target geometry used in these calculations is shown in Fig. 2. The target consists of a cylinder of hydrogen which has a radius r_h and a length L . The hydrogen is enclosed in a cylindrical shell made of solid lead which has a density of 11.3 g/cm³ and which has an outer radius, r_o .

The right face of the target is irradiated with a hollow heavy ion beam which has an annular (ring shaped) focal spot with an inner radius, r_1 and an outer radius, r_2 . The target and the beam parameters are chosen in such a way that r_1 is larger than r_h which avoids direct heating of the hydrogen region by the ion beam and the energy is only deposited in a part of the lead shell around the hydrogen layer. Moreover the target length is chosen to be much less than the ion range in lead so that the ions lose a part of their energy in the target and emerge from the opposite (left) face of the cylinder with a reduced energy. This is a so-called “sub-range” target.

The Bragg peak does not lie inside the target and the energy deposition is uniform along the particle trajectory in the absorption region. A shell of heated material is thus created around the hydrogen region and the high pressure in this hot zone slowly implodes the hydrogen to very high densities and ultrahigh pressures while the temperature remains relatively low.

The preliminary design studies indicate that a maximum number of 2×10^{12} particles of uranium with a wide range of particle energy (400 MeV/u–2.7 GeV/u) will be delivered by the SIS100 facility in a single bunch with corresponding bunch length in the range of 90–20 ns, respectively.

In this study we assume that the particle energy is 2.7 GeV/u and the inner radius of the focal spot ring is, $r_1 = 0.6$ mm while the outer radius is $r_2 = 1.6$ mm. The deposition profile along the radial direction is assumed to be parabolic. The temporal beam power profile is also assumed to be parabolic given by

$$P(t) = -\frac{6E}{\tau^3} [t^2 - \tau t] \quad (1)$$

where E is the total energy in the beam and in this case is about 200 kJ. The duration of the pulse, τ , is assumed to be 20 ns.

The target length L is assumed to be 1.0 cm and the outer radius of the lead shell is 3.0 mm. The radius of the hydrogen region, $r_h = 0.4$ mm.

The specific power deposition by the ion beam into the target material is an important parameter as it determines the final achievable temperature in the material. This parameter is defined by

$$P_s = \frac{E_s}{\tau}, \quad (2)$$

where τ is the pulse duration and E_s is the specific energy deposition given by

$$E_s = \frac{\frac{1}{\rho} \frac{dE}{dx} N}{\pi r_b^2}. \quad (3)$$

In the above equation, $(1/\rho)(dE/dx)$ is the specific energy loss due to a single ion, N is the total number of particles in the bunch, and r_b is the beam radius. At the future SIS100 facility, the beam intensity is expected to increase gradually as a result of optimization of the accelerator parameters over a few years. We therefore considered different values for the beam intensity, N including 10^{11} , 2×10^{11} , 4×10^{11} , 6×10^{11} , 8×10^{11} , and 10^{12} respectively. Our simulations show that the specific energy deposition in the lead absorption region for the above values of N has respective values of 4.7, 9.36, 18.7, 28.03, 37.33, and 46.64 kJ/g. These values of specific energy deposition create temperatures of 2.3, 3.76, 5.7, 7.0, 8.12, and 9.05 eV, respectively. One may therefore use the cold energy deposition data in such a case and we use the SRIM code³² for this purpose. According to this stopping model the range of the 2.7-GeV/u uranium ions in solid lead is 5.95 cm. This leads to a very uniform energy deposition along the particle trajectory through the target because the target length is only 1 cm. It is also to be noted that using different beam intensities, one may access different regions of the phase diagram.

IV. SIMULATION RESULTS

This section presents the numerical simulation results of compression of the multilayered target shown in Fig. 2 using the target and the beam parameters given in Sec. III. These simulations have been carried out using a two-dimensional hydrodynamic model, BIG-2.¹⁶ This code uses an arbitrary Lagrangian-Eulerian method that combines both the Lagrangian and Eulerian approaches. It is based on a Gudonov type scheme that has a second order accuracy in space for solving hydrodynamic equations. It employs a rectangular grid and uses a sophisticated EOS data described elsewhere.^{33,34} The code includes the electron thermal conduction, although this energy transport mechanism does not play any important role under the physical conditions considered in this problem. The code also includes the energy

deposition of the incident ions taking into account the beam geometry.

Figure 2 shows that a hollow intense beam of 2.7-GeV/u uranium particles is incident on the right face of the cylindrical target that consists of a cylinder of hydrogen which is enclosed in a shell of solid lead. We assume that the radius of the hydrogen is $r_h = 0.4$ mm. The outer radius of the lead shell is 3.0 mm while the cylinder length $L = 1.0$ cm. According to the SRIM code,³² the range of 2.7-GeV/u uranium ions in cold solid lead is of the order of 5.95 cm; therefore, the energy deposition along the target length will be fairly uniform.

The beam has a hollow geometry and has an annular or a ring shape focal spot. The inner radius of the focal spot ring is, $r_1 = 0.6$ mm, while the outer radius is, $r_2 = 1.6$ mm, so that the thickness of the focal spot ring is 1.0 mm. It has been shown theoretically³⁵ as well as experimentally³⁶ that such a hollow beam can be produced using a plasma lens. Another option to generate such an annular focal spot is to employ a radio frequency wobbler that can rotate the beam at an appropriate frequency. GSI is also studying the design of such a wobbler and analytic modeling has shown that to have an irradiation asymmetry of a few percent at the target, the rotation frequency should be of the order of a few GHz,³⁷ which is feasible from the technological point of view.

In a previous paper¹⁰ we showed that employing the beam-target geometry shown in Fig. 2, if one uses frozen hydrogen in the target, one may achieve low entropy compression of the hydrogen as a result of multiple shock reflections that occur between the target axis and the tamper. We considered the beam parameters that will be available at the future GSI accelerator facilities including the upgraded SIS18 as well as the new SIS100. It was shown that as result of this implosion scheme one would achieve hydrogen density above 1 g/cm^3 , pressure in the range of 5–10 Mbar. and a temperature of a few thousand K. These are the theoretically predicted physical conditions for hydrogen metallization. In this study we used the SESAME EOS data for hydrogen.

To study the sensitivity of the compression results to the

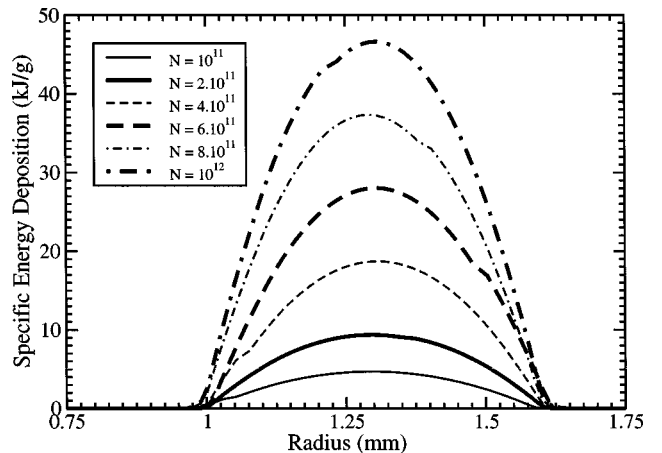


FIG. 3. Specific energy deposition in the lead shell vs the target radius at $t = 20$ ns at $L = 0.5$ mm using different beam intensities noted in Sec. III.

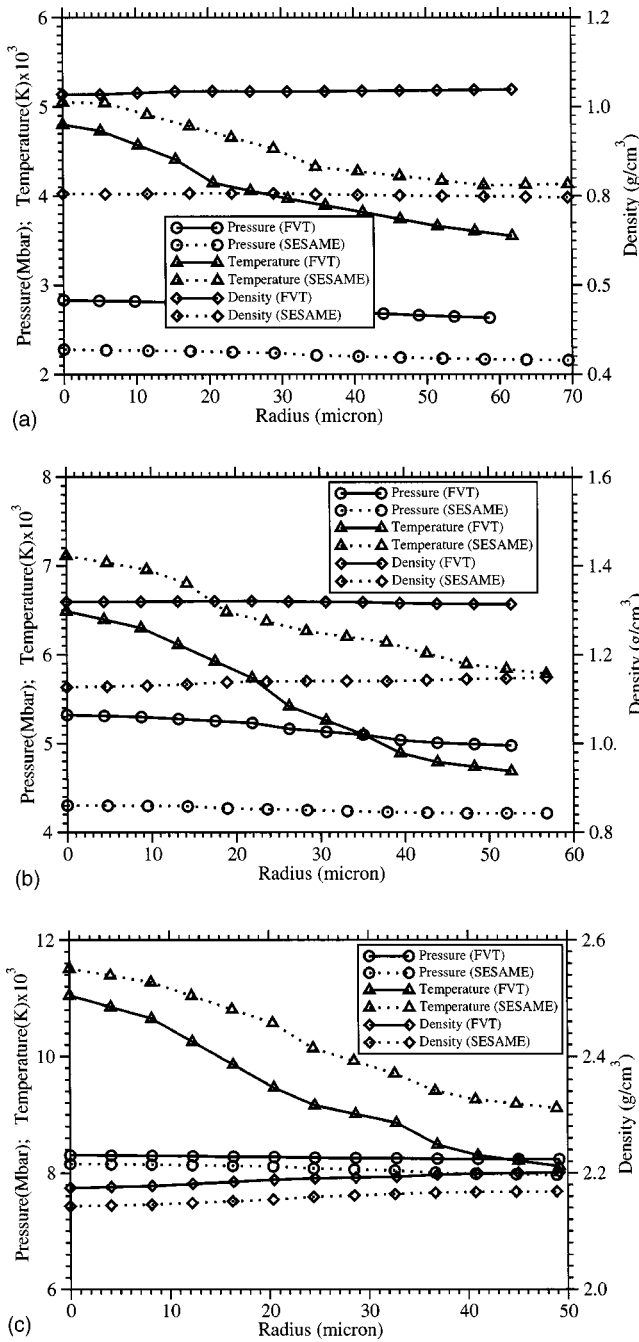


FIG. 4. (a) Hydrogen density, pressure and temperature vs radius at the time of maximum compression assuming an $N=10^{11}$ and using two different EOS models. (b) Same as in (a), but using $N=2 \times 10^{11}$. (c) Same as in (a), but using $N=4 \times 10^{11}$.

EOS model, in the present paper we present results using our EOS model described in Sec. II. However our model can only treat neutral fluid phase using a FVT and the plasma phase using the Padé approximation but cannot treat the solid phase at very low temperatures. Therefore to compare the two models we do not use frozen hydrogen in these calculations but we consider hydrogen at one tenth of solid density at room temperature. In the following we present the simulation results.

In Fig. 3 we plot the specific energy deposition vs target

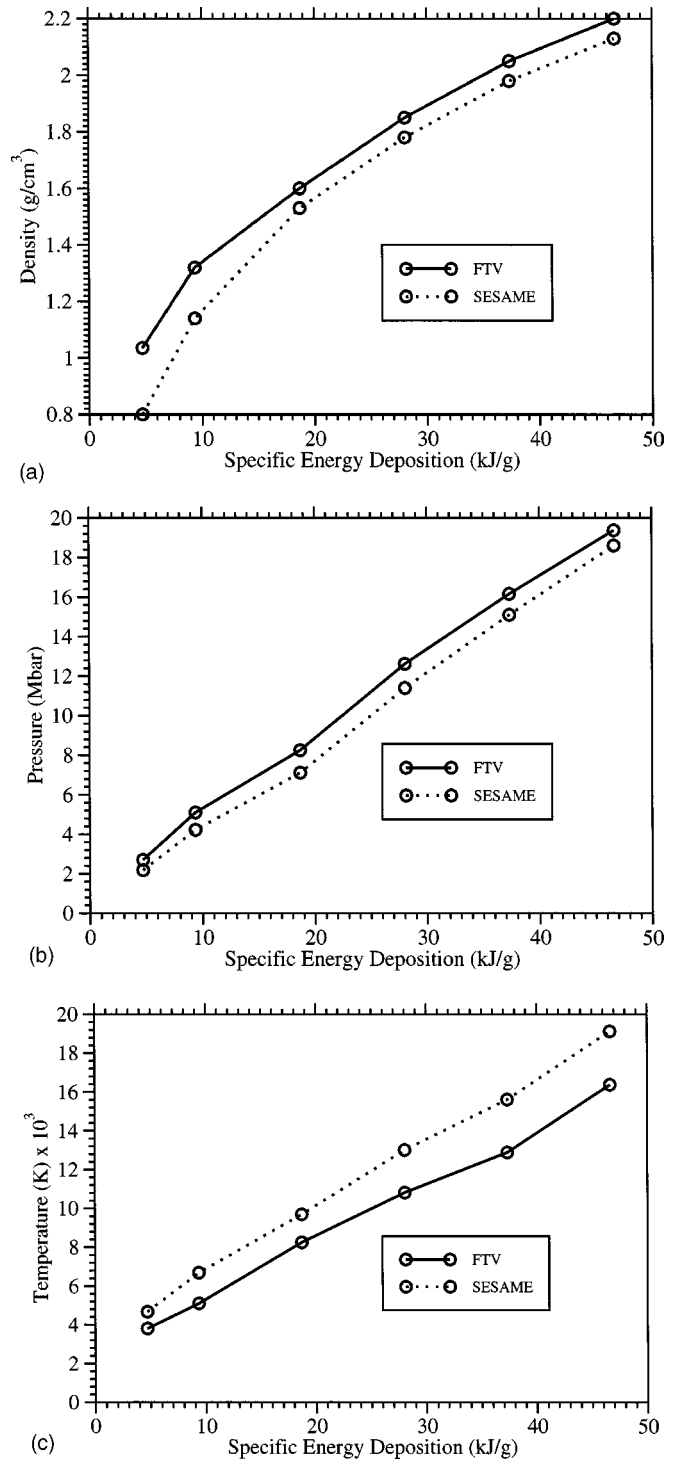


FIG. 5. (a) Hydrogen density vs input energy at the time of maximum compression. (b) Hydrogen pressure vs input energy at the time of maximum compression. (c) Hydrogen temperature vs input energy at the time of maximum compression.

radius at the middle of the target ($L=0.5$ cm), at $t=20$ ns, a time when the beam has just delivered its total energy; for six different values of the beam intensity given in Sec. III. The parabolic nature of the energy deposition along the radial direction is shown in this figure. It is seen that the peak values of the specific energy deposition in these different

cases are 4.7, 9.35, 18.7, 28.03, 37.33, and 46.64 kJ, respectively.

In Fig. 4(a) we plot the density, pressure and the temperature vs target radius in the middle of the target at $L = 0.5$ cm for the case of the lowest driving energy, namely, 4.7 kJ/g using the two EOS models. These results are plotted at the time of maximum compression. It is seen that the average density in case of our model is slightly above 1 g/cm^3 while in case of the SESAME model it is about 0.8 g/cm^3 , a difference of 20%. The pressure also shows the same behavior and is 2.9 Mbar in the case of our model, while for the SESAME model it is about 2.3 Mbar. The temperature, on the other hand, shows an opposite behavior: higher in the case of the SESAME model as compared to our model. The reason is as follows. We believe that in our model, the treatment for molecular dissociation and atomic ionization is more advanced than that used in the SESAME model. Our treatment requires more energy for these processes to take place. As a result of this, during the early stages of compression, more input energy is consumed by these processes in our model which leads to a lower temperature and lower pressure. As a consequence, one achieves a higher final compression which leads to a higher final pressure while the final temperature remains low.

In Figs. 4(b) and 4(c) we plot the same variables as in Fig. 4(a), but using a driving energies of 9.35 and 18.7 kJ/g, respectively. It is seen that as the driving energy is increased, the differences in the results decrease. This is due to the fact that if the driving energy is low, a larger fraction of the input energy is used by the processes of dissociation and ionization, but as the input energy is increased this fraction becomes smaller and smaller and the two models predict similar results.

This is an interesting result which suggests that one would not have to wait until one achieves the full intensity of the SIS100 beam, but interesting physical effects can be studied using at intensity that is an order of magnitude below the maximum design value of 2×10^{12} particles/bunch.

In Figs. 5(a), 5(b), and 5(c) we plot the average density, average pressure and average temperature in the hydrogen region at the time of maximum compression vs the specific energy E_s deposited in the lead absorber. It is seen that as the driving energy increases, the final density increases while the differences in the results predicted by the two EOS models decrease. For the highest value of the driving energy we achieve a density of above 2 g/cm^3 for both cases. Figure 5(b) shows that the average pressure achieved using the maximum driving energy is of the order of 20 Mbar. Figure

5(b) shows that the average temperature for the SESAME case is about 19 000 K while for the case of our EOS model one achieves an average temperature of 16 000 K.

These calculations show that using different beam intensities that will be available at the future SIS100 facility, one may access a wide range of physical parameters that represent different interesting regions of the hydrogen phase diagram. In these calculations we have used one tenth of the solid hydrogen density. The initial hydrogen density is another important parameter that one can vary to extend the region of the achievable physical conditions.

We also note that due to the initial low density of hydrogen used in these calculations, the final temperature is quite high due to strong shock heating. These calculations therefore suggest that such an arrangement will not lead to creation of metallic hydrogen, but is very suitable to study the PPT. In order to study the problem of hydrogen metallization one needs to start with solid hydrogen at a temperature of the order of 10 K, which is intended for the future work.

V. CONCLUSIONS

This paper shows, with the help of two-dimensional hydrodynamic simulations, that intense beams of energetic heavy ions can be used as an efficient tool to compress extended and large volumes of hydrogen in a multi-layered target. We have assumed that a solid lead shell is filled with hydrogen at a density of one tenth of the solid density at room temperature. Two different EOS models, namely SESAME and a model based on FVT+PA, have been used in these calculations. Moreover different values for the beam intensity, N including 10^{11} , 2×10^{11} , 4×10^{11} , 6×10^{11} , 8×10^{11} , and 10^{12} have been considered. It has been found that use of these different beam intensities lead to a very wide range of hydrogen physical conditions that belong to interesting regions of the hydrogen phase diagram. These calculations therefore suggest that these regions can be accessed in the future GSI experiments and an experimental investigation of these states will be a very valuable contribution to this field. It has also been found that our EOS model based on FVT+PA predicts a softer behavior as compared to the SESAME if one uses low driving energies, and the differences disappear if the driving energy is very high.

ACKNOWLEDGMENTS

The authors wish to thank the German Ministry of Research and Development (BMBF) for providing financial support to carry out this work.

¹E. Wigner and H. B. Huntington, J. Chem. Phys. **3**, 764 (1935).

²C. Narayan, H. Luo, J. Orlof, and A. L. Ruoff, Nature (London) **393**, 46 (1998).

³H. K. Mao and R. J. Hemley, Rev. Mod. Phys. **66**, 671 (1994).

⁴S. T. Weir, A. C. Mitchell, and W. J. Nellis, Phys. Rev. Lett. **76**, 1860 (1996).

⁵W. J. Nellis, A. C. Mitchell, P. C. McCandless, D. J. Erskine, and

S. T. Weir, Phys. Rev. Lett. **68**, 2937 (1992).

⁶V. E. Fortov, V. Ya. Ternovoi, S. V. Kvitov, V. B. Mintsev, D. N. Nikolaev, A. A. Pyalling, and A. S. Filimonov, Pis'ma Zh. Eksp. Teor. Fiz. **69**, 926 (1999) [JETP Lett. **69**, 926 (1999)].

⁷V. Ya. Ternovoi, A. S. Filiminov, V. E. Fortov, S. V. Kvitov, D. N. Nikolaev, and A. A. Pyalling, Physica B **265**, 6 (1999).

⁸P. M. Celliers, G. W. Collins, L. B. Da Silva, D. M. Gold, R.

- Cauble, R. J. Wallace, M. E. Foord, and B. A. Hammel, *Phys. Rev. Lett.* **84**, 5564 (2000).
- ⁹R. Cauble, P. M. Celliers, G. W. Collins, L. B. Da Silva, D. M. Gold, M. E. Foord, K. S. Budil, R. J. Wallace, and A. Ng, *Astrophys. J.* **127**, 267 (2000).
- ¹⁰N. A. Tahir *et al.*, *Phys. Rev. E* **63**, 016402 (2001).
- ¹¹G. I. Kerley, in *Molecular Based Studies of Fluids*, edited by J. M. Haile and G. A. Mansoori (American Chemical Society, Washington, DC, 1983), p. 107.
- ¹²L. B. Da Silva *et al.*, *Phys. Rev. Lett.* **78**, 483 (1997).
- ¹³H. Juranek, R. Redmer, and W. Stolzmann, *Comments Condens. Matter Phys.* **41**, 131 (2001).
- ¹⁴H. Juranek and R. Redmer, *J. Chem. Phys.* **112**, 3780 (2000).
- ¹⁵W. Ebeling and W. Richert, *Comments Condens. Matter Phys.* **25**, 431 (1985).
- ¹⁶V. E. Fortov *et al.*, *Nucl. Sci. Eng.* **123**, 169 (1996).
- ¹⁷D. H. H. Hoffmann, K. Weyrich, H. Wahl, D. Gardes, R. Bimbot, and C. Fleurier, *Phys. Rev. A* **42**, 2313 (1990).
- ¹⁸S. Stöwe, R. Bock, M. Dornik, P. Spiller, M. Stetter, V. E. Fortov, V. Mintsev, M. Kulish, A. Shutov, V. Yakushev, B. Sharkov, A. Golubev, B. Bruynetkin, U. Funk, M. Geissel, D. H. H. Hoffmann, and N. A. Tahir, *Nucl. Instrum. Methods Phys. Res. A* **415**, 384 (1998).
- ¹⁹D. Varentsov, P. Spiller, U. N. Funk, D. H. H. Hoffmann, A. Kozyreva, N. A. Tahir, C. Constantin, E. Dewald, J. Jacoby, U. Neuner, S. Udrea, and R. Bock, *Nucl. Instrum. Methods Phys. Res. B* **174**, 215 (2001).
- ²⁰G. I. Kerley, Los Alamos scientific laboratory of the University of California report LA-4776, UC-34, available at National Technical Information Service, U.S. Department of Commerce, 6285 Port Royal Road, Springfield, Virginia 22151.
- ²¹M. Ross, *Phys. Rev. B* **58**, 669 (1998).
- ²²D. Saumon and G. Chabrier, *Phys. Rev. A* **46**, 2084 (1992).
- ²³M. D. Knudson *et al.*, *Phys. Rev. Lett.* **87**, 225501 (2001).
- ²⁴M. Ross, F. H. Ree, and D. A. Young, *J. Chem. Phys.* **79**, 1487 (1983).
- ²⁵G. A. Mansoori, N. F. Carnahan, K. E. Starling, and T. W. Leland, *J. Chem. Phys.* **54**, 1532 (1971).
- ²⁶W. Stolzmann and T. Blöcker, *Astron. Astrophys.* **361**, 1152 (2000).
- ²⁷D. Beule *et al.*, *Phys. Rev. B* **59**, 14 177 (1999).
- ²⁸D. Beule *et al.*, *Phys. Rev. B* **63**, 060202 (2001).
- ²⁹S. Kuhlbrodt and R. Redmer, *Phys. Rev. E* **62**, 7191 (2002).
- ³⁰D. Saumon, G. Chabrier, and H. M. Van Horn, *Astrophys. J., Suppl.* **99**, 713 (1995).
- ³¹D. Saumon, G. Chabrier, D. J. Wagner, and X. Xie, *High Press. Res.* **16**, 331 (2000).
- ³²J. F. Ziegler, J. P. Biersack, and U. Littmark, *The Stopping and Ranges of Ions in Solids* (Pergamon, New York, 1996).
- ³³A. V. Bushman and V. Fortov, *Wide-Range Equation of State for Matter Under Extreme Conditions*, *Sov. Tech. Rev. B, Therm. Phys. Vol. 1* (Harwood, London, 1987).
- ³⁴I. V. Lomonosov, A. V. Bushman, and V. E. Fortov, in *High-Pressure Science and Technology*, edited by S. C. Schmidt, J. W. Schaner, G. A. Samara, and M. Ross (AIP, New York, 1994), Pt. 1, p. 47.
- ³⁵N. A. Tahir, D. H. H. Hoffmann, A. Kozyreva, A. Shutov, J. A. Maruhn, U. Neuner, A. Tauschwitz, P. Spiller, and R. Bock, *Phys. Rev. E* **62**, 1224 (2000).
- ³⁶U. Neuner, R. Bock, M. Roth, P. Spiller, C. Constantin, U. N. Funk, M. Geissel, S. Hakuli, D. H. H. Hoffmann, J. Jacoby, A. Kozyreva, N. A. Tahir, S. Udrea, D. Varentsov, and A. Tauschwitz, *Phys. Rev. Lett.* **85**, 4518 (2000).
- ³⁷A. R. Piriz, N. A. Tahir, D. H. H. Hoffmann, and M. Temporal, *Phys. Rev. E* **67**, 017501 (2003).